Proceedings of The Institute of Acoustics

MODELS FOR EVALUATING THE PERFORMANCE OF PROPELLER AIRCRAFT ACTIVE NOISE CONTROL SYSTEMS

A.J. Bullmore, P.A. Nelson, S.J. Elliott

Institute of Sound and Vibration Research
University of Southampton, Southampton SO9 5NH, England.

INTRODUCTION

The application of active noise control to the reduction of propeller-induced cabin noise has been the subject of several recent papers [1-7]. Most of these works have addressed the problem at a fundamental level in order to best illustrate the physical mechanisms by which the active control of harmonic enclosed sound fields is effected. As a result of such work it has been established that active noise control can be used to produce reductions in the level of enclosed sound fields, both in a "global" sense and in a "local" sense. The dominant parameter controlling the levels of reduction which may be obtained using a given control system has been shown in reference [8] to be the relative contributions of the acoustic modes to the total energy of the sound field (this is a function of the operating frequency, the size of the enclosure, acoustic damping and the spatial extent of the primary source distribution.

If a theoretical model is to accurately predict the levels of reduction which can be achieved using an active noise control system in practice, then the sound field must be modelled accurately. In the case of the rectangular enclosed sound fields of reference [10] it was relatively easy to obtain the required accuracy in modelling the sound field. However, due to the complex acoustic and structural properties of an aircraft cabin the situation addressed in this paper is not so straightforward. Any model capable of producing accurate pointwise predictions of the sound pressure field in an aircraft cabin would involve complex numerical techniques and, in addition, an extensive series of experimental measurements to determine the input parameters to these numerical models. If, however, one can develop a theoretical model which can predict the general features of the acoustic field within an aircraft cabin, and in particular if this model accurately reflects the acoustic damping, the acoustic modal density and the extent of the primary source (fuselage wall/trim) vibration present in the real aircraft, then its use to predict the performance of active noise control should give overall results which are representative of what will occur in practice. Of course, pointwise predictions of either the primary pressure field or the reductions obtained cannot be expected.

The work reported in this paper describes the use of highly idealised theoretical models to represent the structural and acoustic response of a B.Ae. 748 aircraft cabin at the first two propeller blade passage harmonic frequencies (88 Hz and 176 Hz). The use of such a simple model is justified and two illustrative examples of the theoretical application of active noise control to this aircraft are presented.

MODELS FOR EVALUATING THE PERFORMANCE OF PROPELLER AIRCRAFT ACTIVE NOISE CONTROL SYSTEMS

THE CHOICE OF A SIMPLIFIED ANALYTICAL MODEL OF THE AIRCRAFT CABIN STRUCTURAL AND ACOUSTICAL RESPONSE

The Fuselage Structural Response Model

In the theory used in reference [1] the fuselage structural response was modelled as the response of a finite, isotropic, cylindrical shell having shear diaphragm/shear diaphragm end conditions (see Figure 1). The same theory is to be used in the current work.

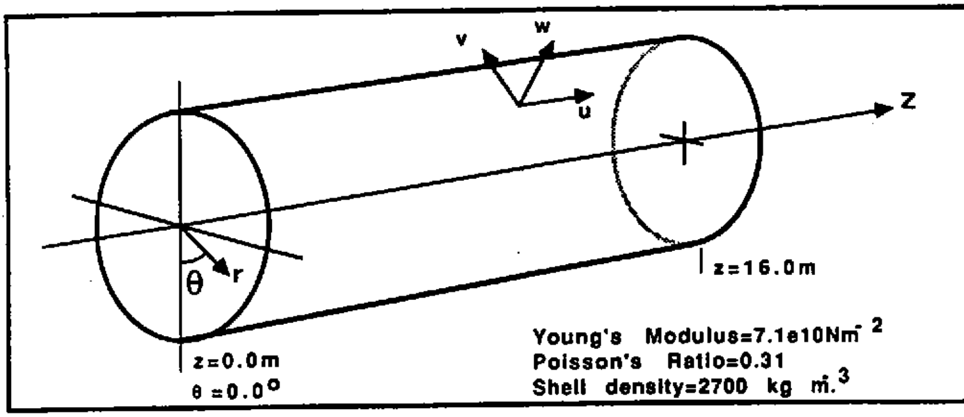

FIGURE 1. Schematic diagram of the shell showing the coordinate system used.

Thus, assuming harmonic excitation, the radial shell displacement $w(z,\theta)$ is evaluated using

$$w(z,\theta) = \sum_{r_1=0}^{R_1}\sum_{r_2=0}^{R_2}\sum_{r_3=0}^{1} \frac{\epsilon_{r_2} a(1-\nu^2) I_{33}}{\pi L_z E(1 + j\eta_s)h}$$

$$. I_r^f \sin\left(\frac{r_1\pi z}{L_z}\right)\cos\left(r_2\theta - \frac{r_3\pi}{2}\right)e^{j\omega t}$$

$$\epsilon_\nu = 1,\quad \nu = 0 \quad \text{or} \quad \epsilon_\nu = 2,\quad \nu > 0 \qquad (1)$$

where a is the shell radius, L_z the shell length and h the shell thickness, r_1, r_2 and r_3 are structural modal integers, E and ν are the shell material Young's modulus and Poisson's ratio respectively and η_s is the hysteretic damping factor. I_r^f specifies the spatial coupling between the applied force and the mode r (where r is used here to indicate the trio of numbers r_1, r_2 and r_3), thus

$$I_r^f = \int_0^{2\pi}\int_0^{L_z} P_f(z,\theta)\sin(\frac{r_1\pi z}{L_z})\cos(r_2\theta - \frac{r_3\pi}{2})a\,dz\,d\theta \qquad (2)$$

where $P_f(z,\theta)$ is the externally applied pressure. The term I_{33} in equation (1) is evaluated as the (3,3) element of the inverse of the 3 × 3 matrix whose elements are given by

$$L_{11} = \Omega^2 - k_z^2a^2 - (\frac{1-\nu}{2})r_2^2$$

$$L_{12} = (\frac{1+\nu}{2})r_2k_za = L_{21}$$

$$L_{13} = \nu k_za = L_{31}$$

$$L_{22} = \Omega^2 - (\frac{1-\nu}{2})(1+\beta^2)k_z^2a^2 - (1+\beta^2)r_2^2 \qquad (3)$$

$$L_{23} = -r_2 - \beta^2(k_z^2a^2n + n^3) = L_{32}$$

$$L_{33} = \Omega^2 - 1 - \beta^2(k_z^4a^4 + 2k_z^2a^2r_2^2 + r_2^4)$$

where $k_z = (r_1\pi/L_z)$ and where $\Omega = (\rho_s a^2(1-\nu^2)\omega^2/E)^{1/2}$ is the non-dimensional frequency which has been normalized to equal unity at the shell ring frequency, ω_r, (so $\Omega = \omega/\omega_r$), ρ_s is the density of the shell material and β is a non-dimensional thickness parameter given by $\beta^2 = (h^2/12a^2)$.

Whilst this basic approach of modelling the fuselage structural response as a finite, isotropic cylindrical shell will remain identical in the present work to the approach used in reference [1], it is now intended to apply the theoretical results to a specific aircraft. The aircraft to be considered is a British Aerospace 748, twin turboprop, 48 seat aircraft. Therefore the dimensions of the shell must be adapted to match the dimensions of the aircraft. Following the arguments presented in references [7,8 and 9] a shell of length 16.0 m and diameter 2.6 m would appear to be appropriate. This corresponds to a cylinder extending from z = 0.0 m at the front of the flight deck to z = 16.0 m at the rear of the galley compartment. The propeller plane is located at z = 3.5 m and the volume corresponding to the 48 seat passenger compartment extends from z = 3.5 m to z = 12.5 m. The shell material is chosen to have the properties of aluminium, as listed in Figure 1.

Structural Response Model Validation

In order to use the theoretical model described in the previous section with any confidence it is necessary to validate the results of the model with those obtained in practice. However, during this validation procedure it must be remembered that one is only looking to achieve general agreement between the experiment and theory.

The model validation was performed using in-flight experimental data measured on a B.Ae.748 test aircraft and made available by British Aerospace plc. Unfortunately, due to the space limitations, only a representative sample of these results can be presented. More detailed results can be found in references [7,8,9].

Because the available experimental data for performing this matching were all measured in flight, it is necessary to ensure that the forcing used in the theoretical model demonstrates the important features of the in-flight forcing of the fuselage. This is particularly important as results presented in reference [9] have shown the forced response of a shell such as that described above to be heavily dependent on the exact form of the forcing. In particular, the distributed nature and the circumferential convection of the pressure field have been shown to be important parameters controlling the response of the structure. Thus, based on experimental data, the pressure fields shown in Figure 2 were chosen. (Note the absolute levels of these results, and all subsequent results, have been scaled to 94 dB peak).

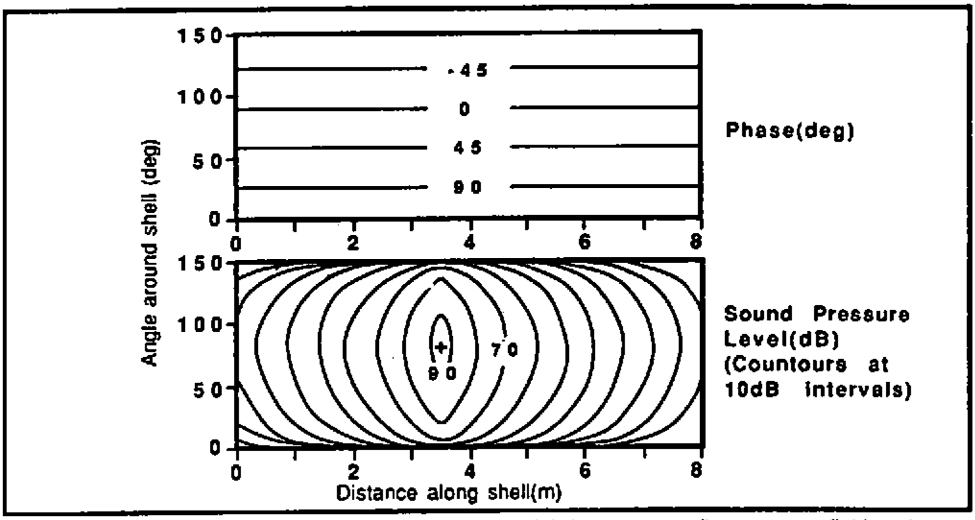

FIGURE 2. The external pressure field used to model the port propeller pressure field at the blade passage first harmonic frequency. The peak sound pressure level is 94dB at "+". The second harmonic pressure field is of the same form except the peak pressure level is 91.4dB and the circumferential phase rate is double that of the first harmonic.

Using the shell thickness, h, and damping η_s, as variables, the predicted structural responses were "matched" with the available experimental structural response data. This resulted in the shell thickness being chosen as 1.2 mm, and the hysteretic damping factor as 0.3. Figure 3 shows the scaled structural radial acceleration amplitudes at 88 Hz due to the port propeller only. Figure 3(a) shows the response as a function of distance along the fuselage evaluated and measured on a line along the port side of the fuselage, this line intersecting the point of closest approach of the propeller. Figure 3(b) shows the response as a function of angle around the fuselage in the plane of the propellers.

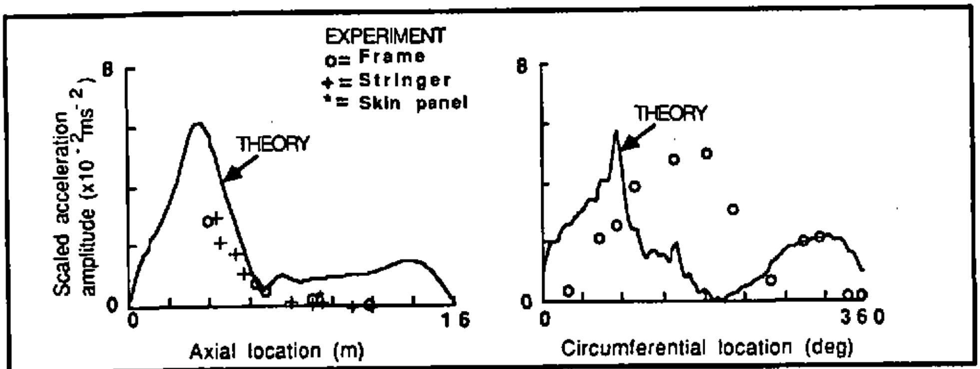

FIGURE 3. The radial acceleration amplitude of the shell at 88Hz when it is excited by the pressure field of Figure 2. Some experimentally measured data points are also shown for comparison.

From the results of Figure 3(a) it appears that, whilst the theory predicts the nature of the responses along the shell with reasonable agreement, the predicted acceleration amplitudes are too high. The reason for this can be seen by referring to the responses around the shell shown in Figure 3(b). For this case the maximum amplitudes of the experimental and theoretical results show good agreement. However, the theoretical results predict that the maximum response occurs close to the point lying under the maximum applied pressure (i.e., at z = 3.5 m, θ = 85°). In contrast, the experimental responses appear to be rotated around the fuselage in the direction of the propeller rotation. Thus, the peak measured acceleration occurs at θ = 180°. The reason for this behaviour is not clear but it is possibly due to the constraints imposed on the fuselage vibration by the floor. However, the effect does explain the overprediction of the acceleration amplitudes in Figure 3(a).

From these and other similar results it was concluded that the finite shell theory, with the appropriately chosen parameters, could be used to provide a realistic primary source distribution for use in the active noise control prediction scheme.

The Cabin Acoustic Response Model

The work presented in reference [1] chose to model the cabin sound field as that which exists in a hard-walled cylindrical room. It is the intention in this section to assess how good a model this is.

MODELS FOR EVALUATING THE PERFORMANCE OF PROPELLER AIRCRAFT ACTIVE NOISE CONTROL SYSTEMS

The acoustic pressure at a point specified by the location vector $\underline{r}$, due to some normal velocity distribution $v_n(\underline{r}_s,\omega)$ over the cylinder walls can be expressed as (see Figure 1 for the cylindrical coordinate system used) [8]

$$p(\underline{r},\omega) = \frac{\omega\rho c^2}{V} \sum_{n=0}^{N} \frac{\psi_n(\underline{r})\int_s v_n(\underline{r}_s,\omega)\psi_n(\underline{r}_s)dS}{2C_n\omega_n - j(\omega_n^2 - \omega^2)} \qquad (4)$$

where harmonic time dependence of frequency ω has been assumed. Here ω_n and ψ_n are the natural frequency and normalised mode shape functions of the n'th mode given by

$$\omega_n = c\left(\left(\frac{n_1\pi}{L_z}\right)^2 + \left(\frac{k_{n_2n_3}}{a}\right)^2\right)^{1/2} \qquad (5)$$

and

$$\psi_{n_1n_2n_3n_4} = \frac{\cos\left(\frac{n_1\pi z}{L_z}\right)\cos\left(n_2\theta + \frac{n_4\pi}{2}\right)J_{n_2}\left(\frac{k_{n_2n_3}r}{a}\right)}{\Lambda_n^{\frac{1}{2}}} \qquad (6)$$

where n_1, n_2, n_3 and n_4 are the modal integers, L_z is the length of the cylinder J_{n_2} is a Bessel function of order n_2, $k_{n_2n_3}$ are solutions of $(\partial J_{n_2}(k_{n_2n_3})/\partial r) = 0$ and a is the radius of the cylinder. The eigenfunctions have been normalized using

$$\Lambda_n = \frac{1}{\epsilon_{n_1}}\frac{1}{\epsilon_{n_2}}\left(1 - \frac{n_2^2}{k_{n_2n_3}^2}\right)J_{n_2}^2(k_{n_2n_3}) \qquad (7)$$

Also, V and S are the volume and bounding surface area of the enclosed space, ρ and c are the density and sound speed of the enclosed medium, and C_n is the damping constant of the n'th mode, which is related to the surface averaged absorption coefficient by

$$C_n = \frac{c}{16V}\left[S_e\bar{\alpha}_e\epsilon_{n_1} + \frac{S_c\bar{\alpha}_c}{1 - \left(\frac{n_2}{k_{n_2n_3}}\right)^2}\right] \qquad (8)$$

where S_e is the surface area and $\bar{\alpha}_e$ the surface averaged absorption coefficient of the end walls and where S_c and $\bar{\alpha}_c$ are the equivalent quantities for the curved walls. In the work that follows, the distribution of absorbing material over the end and curved walls will be assumed to be equal, and therefore $\bar{\alpha}_e$ will equal $\bar{\alpha}_c$.

MODELS FOR EVALUATING THE PERFORMANCE OF PROPELLER AIRCRAFT ACTIVE NOISE CONTROL SYSTEMS

Acoustic Response Model Validation

To check the applicability of this theory to the physical situation a series of ground tests were performed in the cabin of the trials aircraft. These tests were designed to determine the acoustic damping in the cabin in the frequency range of interest and also to try and identify the modal structure of the sound field. Two methods were explored: steady state power balance techniques and acoustic transfer impedance measurements [8], with a frequency range from 0 to 500 Hz being considered. Table 1 lists the best estimates of acoustic absorption coefficients obtained using a combination of these two methods. Note that the very high absorption coefficients quoted have resulted from the cylinder model having a much smaller surface area than the aircraft cabin where seats, bulkheads, lockers, etc., are present. As with the structural responses, the overall results from these tests indicated that this simple model should adequately describe the acoustic response of the cabin at frequencies up to the second blade passage harmonic [8].

TABLE 1: The acoustic absorption coefficients used in the cylindrical room acoustics model to best match the predicted acoustic responses to the measured values.

Frequency (Hz)	Absorption Coefficient
$f < 25$	0.1
$25 < f < 200$	$f \times 0.008$
$200 < f < 500$	1.6

The next question which must be asked is, when the structural and acoustic response models are interfaced, do they still give results which agree adequately well with practical measurements?

The Combined Fuselage Structural and Cabin Acoustic Response

As the next stage of model validation, the internal acoustic responses due to the predicted shell structural responses were evaluated by substituting the expression for the shell radial velocity from equation (1) into equation (4). Performing this substitution and evaluating the appropriate integrals, assuming the shell end caps to be acoustically rigid, yields the pressure fields of Figure 5, where these fields have been evaluated over the plane shown in Figure 4. These are to be compared with the experimental pressure fields measured over a corresponding plane and shown in Figure 6. Whilst the agreement for the fundamental frequency is reasonable, the agreement for the second harmonic is not so good.

This discrepancy between theory and experiment is believed to occur because of the highly idealized nature of the theoretical model used, and the manner in which the structural response excites the enclosed acoustic field [7].

MODELS FOR EVALUATING THE PERFORMANCE OF PROPELLER AIRCRAFT ACTIVE NOISE CONTROL SYSTEMS

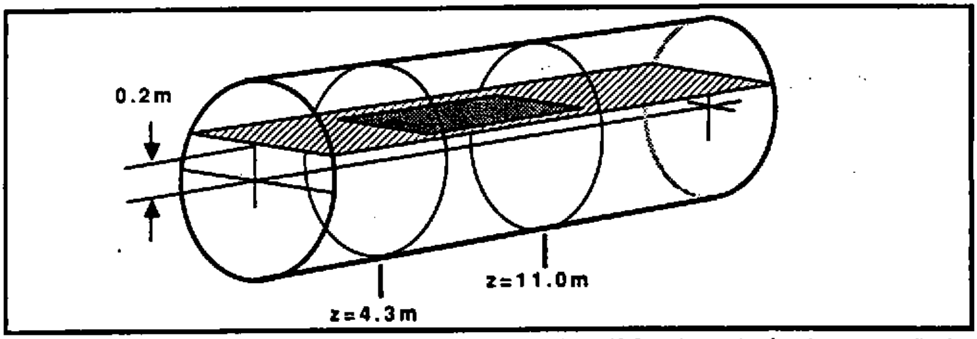

FIGURE 4. Schematic diagram showing the head height plane (0.2m above the fuselage centreline) over which both the experimental and theoretical sound pressure field results have been evaluated. The plane is indicated by the heavy shading.

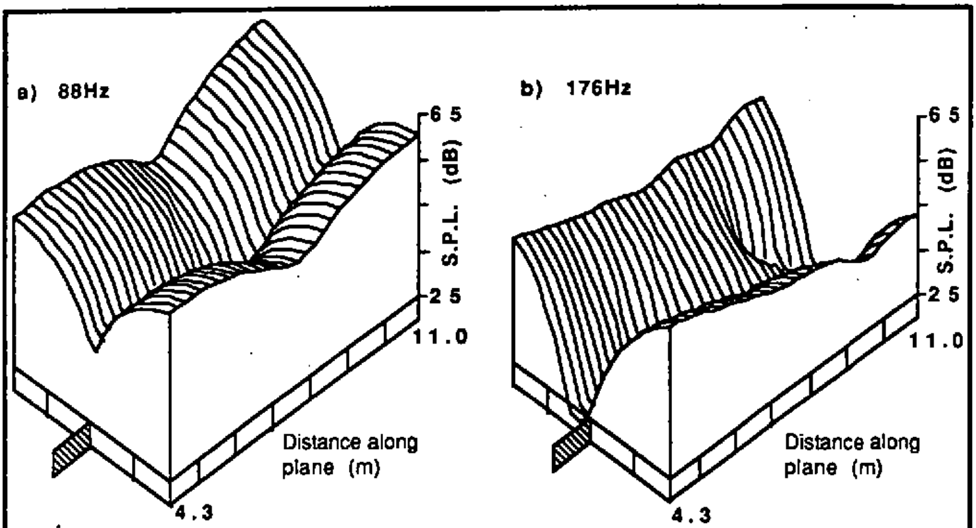

FIGURE 5. The theoretically predicted sound pressure fields over the "seated head height plane" in the shell of Figure 4. The fields shown are due to port propeller excitation only.

The inhomogeneities present in any practical aircraft structure are likely to decrease this structural/acoustic mode coupling selectivity and thus at any given frequency a different combination of modes are likely to be excited than is predicted by this simple theory. In order to introduce this effect into the model (albeit in a rather *ad hoc* manner) the excitation of the enclosed volume by the vibration of the shell can be modified to occur over only part of the interior shell surface. Since the fuselage floor is joined to the cylindrical fuselage at points corresponding approximately to $\theta = 60^\circ$ and $\theta = 300^\circ$, and because there are fixed bulkheads in the test aircraft at

MODELS FOR EVALUATING THE PERFORMANCE OF PROPELLER AIRCRAFT ACTIVE NOISE CONTROL SYSTEMS

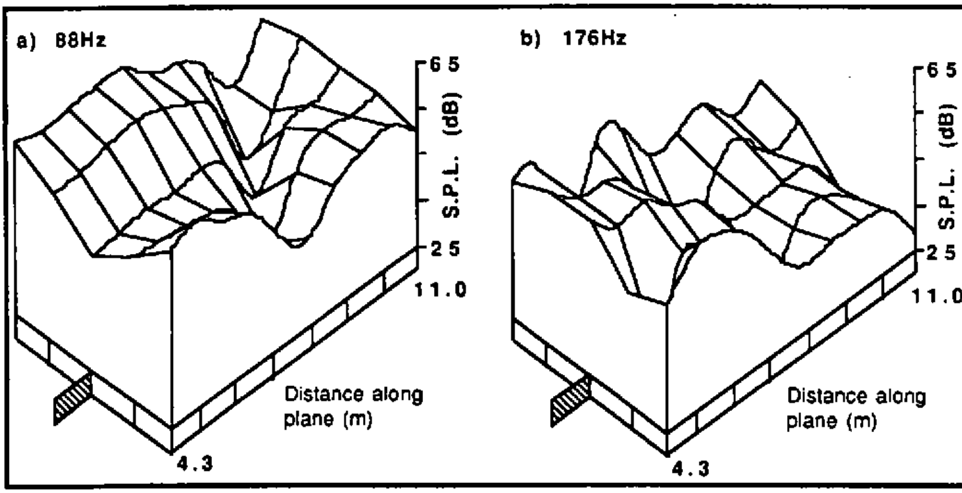

FIGURE 6. The experimentally measured sound pressure fields over the seated head height plane in the passenger cabin of the B.Ae. 748 aircraft. The fields shown are due to the port propeller only and were measured in flight.

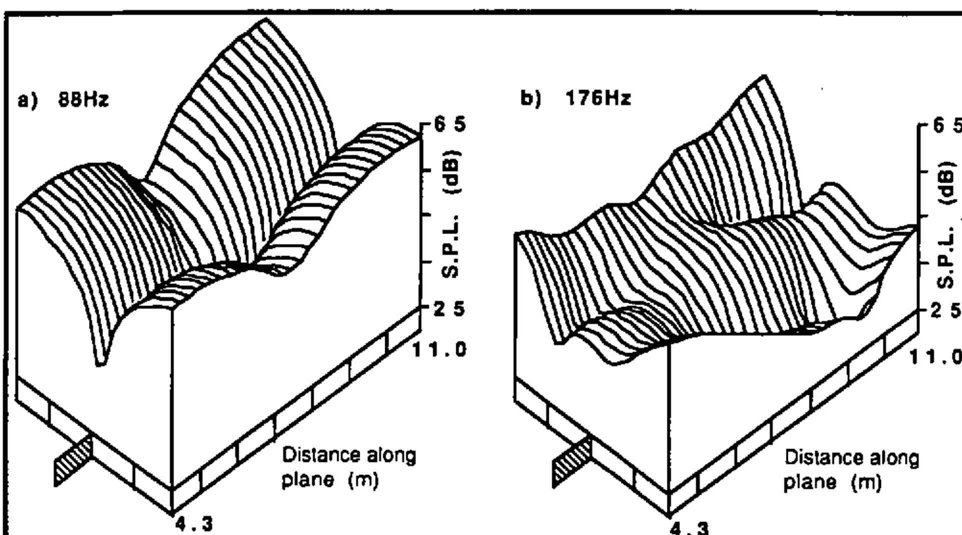

FIGURE 7. The MODIFIED theoretically predicted sound pressure fields over the "seated head height plane" in the shell of Figure 4. The fields shown are due to port propeller excitation only.

approximately $z = 1.5$ m and $z = 12.5$ m, it has been decided to choose these as the limits of the "primary source". Figure 7 shows the pressure distributions resulting from making this modification to the excitation. These pressure fields have again been evaluated over the head height plane of Figure 4. Note that now, particularly at 176 Hz, the predicted and measured responses are in much better agreement.

THE APPLICATION OF ACTIVE NOISE CONTROL AT THE PROPELLER BLADE PASSAGE FIRST AND SECOND HARMONIC FREQUENCIES

The Active Control System Cost Function

The model described above can now be used to predict the levels of reduction which are likely to be achieved using active methods of sound reduction. As a practical method of applying active noise control the technique of minimising the sum of the squared pressures at L error sensors shall be considered. This is the same technique as was used in, for example, references [1,7,8]. Thus the cost function to be minimised is given by

$$J_p = \frac{V}{4\rho c^2 L} \sum_{\ell=1}^{L} |p(\underline{r}_\ell,\omega)|^2$$

where $p(\underline{r}_\ell,\omega)$ is the pressure at the location of the ℓ'th sensor. The method of interfacing an active control performance prediction scheme of this type with analytical acoustics models similar to that described above has been previously described in reference [10] and hence will not be discussed here. However, the basic property of this type of quadratic optimisation analysis is that if one specifies any number, M, and location of secondary sources and any number, $L \geq M$, and location of error sensors then the theoretical analysis allows the prediction of the optimal set of secondary source strengths which will minimise the chosen cost function.

The Secondary Source/Error Sensor Location

Having chosen J_p as a suitable cost function it is now necessary to choose a suitable number and location of both secondary sources and error sensors. As an example of a "practically sized" system, one having 8 secondary sources and 24 error sensors shall be considered. In the low modal density case discussed in reference [10] it was demonstrated that global reductions of up to 20 dB in the total acoustic potential energy within the volume could be achieved using specific combinations of only one or two secondary sources and error sensors. This was made possible by the primary sound field being dominated by only one or two modes. In the present case, however, if one evaluates the number of modes which dominantly contribute to the total acoustic potential energy of the primary sound field (by "dominantly" it is meant the mode's contribution is within 20 dB of the most dominant mode) then at the fundamental frequency 10 modes dominate, and at the second harmonic frequency more than 60 modes dominate. It is thus unlikely that the 8 source/24 sensor active control system will be capable of producing appreciable global reductions. Instead, a strategy which attempts to reduce

MODELS FOR EVALUATING THE PERFORMANCE OF PROPELLER AIRCRAFT ACTIVE NOISE CONTROL SYSTEMS

the sound levels in the regions where reductions are most needed will be adopted. Consequently the twenty four error sensors are spaced evenly over the seated head height plane of Figure 4, resulting in the sensor distribution shown in Figure 8(a). These error sensor locations shall be kept identical for both the fundamental and second harmonic systems. However, the eight secondary source locations used for the two harmonic differ. The two source distributions used are shown on Figures 8(b) and (c). full discussion on the reasons for these choices of source locations can be found in reference [8].

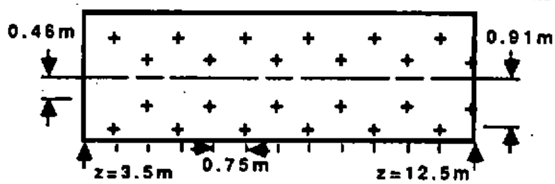

a) The locations of the twenty four error sensors used for both the fundamental and second harmonic frequency active control systems. All sensors are located in the head height plane of Figure 8.

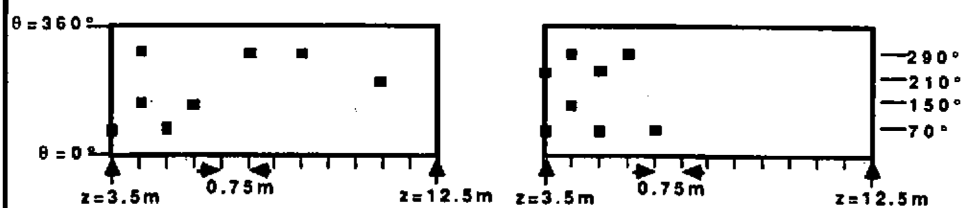

b) The locations of the 8 secondary sources used for the fundamental frequency active control system. The diagram shows the locations over the unwrapped shell surface.

c) The locations of the 8 secondary sources used for the second harmonic frequency active control system. The diagram shows the locations over the unwrapped shell surface

FIGURE 8. The locations of the 8 sources and 24 error sensors used to obtain the results of Figures 9 and 10.

Results for the Propeller Blade Passage First Harmonic Frequency

Figure 9 shows the results of minimising J_p at the blade passage fundamental frequency. The results are presented for a 30 by 20 point grid over a head height plane similar to that shown in Figure 4. Thus the plane includes the error sensor locations. For this case the average reduction over the 600 points in the plane (this quantiy shall be termed J_{p600}) is 8.2 dB, while the average reduction at the 24 error sensors, J_{p24}, is 8.9 dB, and the total acoustic potential energy decreases by less than 0.1 dB. Notice, however, from Figure 9 that local reductions in the sound presure level of up to 35 dB are predicted. Increases of up to 20 dB are also predicted, but these only occur where the pressure was initially very low. The general effect of minimising J_p has therefore been to reduce the average sound pressure level

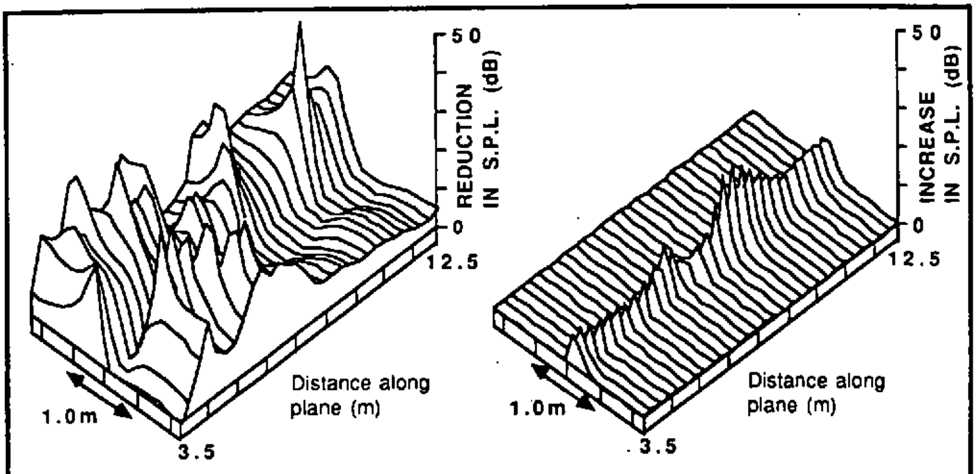

a) Areas of pressure decrease after Jp has been minimised.

b) Areas of pressure increase after Jp has been minimised.

FIGURE 9. The effect over the head height plane of minimising Jp at the propeller blade passage fundamental frequency using the active control system of Figure 8.

over the plane, with the spatial extent around each error sensor being sufficiently large that no significant regions of pressure increase occur between the sensors.

Results for the Propeller Blade Passage Second Harmonic Frequency

Figure 10 shows the corresponding result for the 8 source/24 sensor system operating at the blade passage second harmonic frequency. In this case the reduction in J_{p600} is 2.3 dB, the reduction in J_{p24} is 7.2 dB and the total acoustic potential energy increases by 0.6 dB. The J_{p600} reduction is substantialy less than that obtained at the fundamental frequency. This is partly due to the concentration of the reductions in the forward half of the plane with the average pressure slightly increasing in the rear half of the plane. This is not too detrimental to the practical usefulness of the result as the initial sound pressure levels in the rear half of the plane are, on average, 8 dB lower than those in the forward half. However, the lower J_{p600} reduction is also caused by the zones of reduction being concentrated more closely around the error sensors for the second harmonic frequency results.

What has not been considered in the results of Figures 9 and 10 is the out of plane performance of the active control system. Results in reference [8] show that as one moves vertically away from the plane of the error sensors the reductions obtained using the second harmonic system fall off much more rapidly than those obtained at the fundamental frequency, thus suggesting the need to move the error sensors out of the single "head height" plane. This feature, that the reductions are more localized around the error sensors for the second harmonic frequency, is also demonstrated by the comparison of the $J_{p_{24}}$ and $J_{p_{600}}$ reductions at each of the two harmonics.

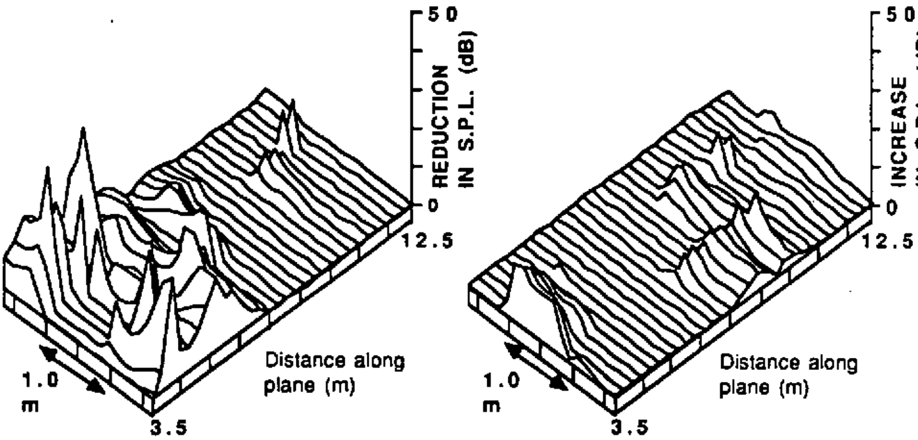

a) Areas of pressure decrease after Jp has been minimised.

b) Areas of pressure increase after Jp has been minimised.

FIGURE 10. The effect over the head height plane of minimising Jp at the propeller blade passage second harmonic frequency using the active control system of Figure 8.

CONCLUSIONS

A simple analytical approach to modelling the structural and acoustic response of a B.Ae.748 aircraft has been presented. Results obtained using this analytical model have been shown to compare well with the general features of the measured aircraft structural and acoustic responses. Having justified the choice of this simplified model it has been used to investigate the application of active noise control within the B.Ae.748 cabin to reduce the interior noise levels at the propeller blade passage fundamental and second harmonic frequencies. The active control system studied comprised 8 sources and 24 error sensors and acted so as to minimise the sum of the squared pressures at the 24 sensors. The possibility of producing global reductions using this size system was considered and rejected. Instead it was attempted to produce an extended area of sound pressure reduction over a seated head height plane which covered all 48 seats. By placing all 24 error sensors in this plane average reductions over the plane of approximately 8 dB at the fundamental frequency and 2 dB at the second harmonic frequency were predicted. However, it has also been demonstrated that the spatial extent of the zones of reductions in sound pressure level are more localized around the error sensors for the second harmonic frequency than for the fundamental frequency.

MODELS FOR EVALUATING THE PERFORMANCE OF PROPELLER AIRCRAFT ACTIVE NOISE CONTROL SYSTEMS

ACKNOWLEDGEMENTS

The authors would like to acknowledge British Aerospace plc for the provision of, and permission to publish, the experimental data. They also wish to acknowledge the Department of Trade and Industry who funded this work.

REFERENCES

1. Bullmore, A.J., Nelson, P.A. and Elliott, S.J. "Active minimisation of acoustic potential energy in harmonically excited cylindrical enclosed sound fields", *Proceedings of the AIAA 10th Aeroacoustics Conference*, 1986, Paper no. AIAA-86-1958.
2. Lester, H.C. and Fuller, C.R. "Active control of propeller induced noise fields inside a flexible cylinder", *Proc. AIAA 10th Aeroacoustic Conference*, 1986, Paper no.AIAA-86-1957
3. Zalas, J.M. and Tichy, J. "Active attenuation of propeller blade passage noise", *NASA CR*-172386, 1984.
4. Ross, C.F. "Active noise control". *Proc. of the 15th Congress of the International Council of Aeronautical Sciences*, 1986, Paper no. ICAS-86-5.8.3, 1986, pp. 1186-1189.
5. Abler, S.B. and Silcox, R.J. "Experimental evaluation of active noise control in a thin cylindrical shell", *Proceedings of Noise Con 87*, 1987, pp. 341-346.
6. Lester, H.C. and Fuller, C.R. "Mechanisms of active control for noise inside a vibrating cylinder", *Proceedings of Noise Con 87*, 1987, pp.371-376.
7. Bullmore, A.J., Nelson, P.A., Elliott, S.J., Evers, J.F., Chidley, B. "Models for evaluating the performance of propeller aircraft active noise control systems". *Proceedings of the AIAA 11th Aeroacoustics Conference*, 1987, Paper No. AIAA-87-2704.
8. Bullmore, A.J. "The active minimisation of harmonic enclosed sound fields with particular application to propeller induced cabin noise". *Ph.D. Thesis*, University of Southampton, 1987.
9. Bullmore, A.J. "A comparison of simple analytical models for representing propeller aircraft structural and acoustic responses". *ISVR Technical Report* No. 153, 1988.
10. Nelson, P.A., Elliott, S.J., Bullmore, A.J., Curtis, A.R.D. "The active minimistion of harmonic enclosed sound fields; Parts I,II and III", *Journal of Sound and Vibration* 117(1), 1987.